

THE ELECTRON FLUX J SENSOR FOR HILAT

The J sensor on the HILAT satellite measures the local flux of electrons over the energy range from 20 to 20,000 electronvolts. Such measurements are important to the HILAT mission since it is the collisional interaction of these particles with the upper atmosphere that is thought to play a major role in the production of F and E region ionization. Irregularities in this ionization can then produce phase and amplitude scintillation of radio signals propagating through the ionization regions.

SENSORS

The J sensor measures the electron flux using an array of six cylindrical curved-plate electrostatic analyzers arranged in three pairs. Figure 1 is a photograph of one such pair. Each analyzer consists of three basic components: an aperturing system, a set of two concentric cylindrical curved plates, and a set of channeltrons.¹ The aperture system collimates the incoming electrons, defining the solid angle over which electrons have access to the space between the cylindrical plates. A potential applied to the plates creates an electric field that causes electrons entering the space between the plates to be accelerated toward the inner plate. If the electron's energy is such that the centrifugal force experienced by the electron as its trajectory is bent by the electric field equals the electric field force, the electron passes along the gap between the plates and impacts the front end of the channeltron.

Each pair of analyzers consists of one set of cylindrical plates with a radius of curvature of 60° and one set with a radius of curvature of 127°. The 127° detector measures electrons in eight semilogarithmically spaced channels between 20 and 632 electronvolts (eV). It has an acceptance angle, full-width-at-half-maximum of approximately 4 by 6°, where the 4° is measured in the plane normal to the edge of the cylindrical plate closest to the aperture assembly and the 6° is measured in the plane parallel to that edge. The 60° detector measures electrons similarly in eight channels between 632 and 20,000 eV, with acceptance angles of 2 by 9°.

RESPONSE CURVES

For a fixed voltage on the cylindrical plates, the detector measures electrons over a solid angle, $\Delta\Omega$, and over an energy passband, ΔE . If the detector response is integrated over all angles at a series of energies for a fixed plate voltage, response curves as shown in Figs. 2 and 3 are obtained. In these figures, the response function for several different voltages on the plates has been normalized to the central energy and peak response. Such response curves, known as the energy-dependent geometric factor, $G(E)$, allow one to relate the pulse counts from the channeltron with a fixed

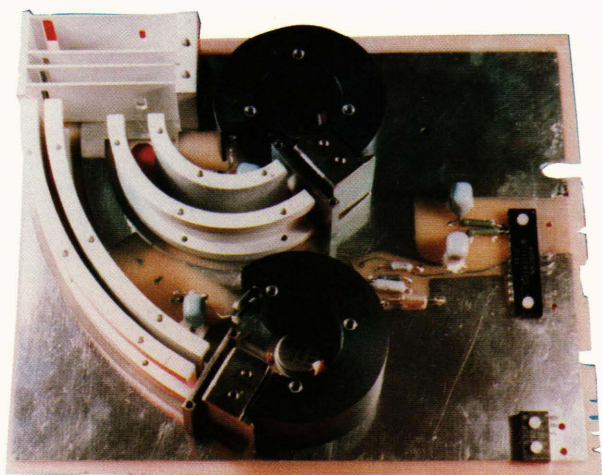


Figure 1—One of the three pairs of analyzers for the HILAT J sensor showing the aperture system, the two sets of cylindrical curved plates (60° and 127°), and the channeltrons with their housing and first stage electronics.

plate voltage to the differential number flux incident at the detector aperture. The equation relating the quantities is

$$j(E) = \frac{CNTS/\Delta T}{G(E_p)\Delta E}$$

where

- $j(E)$ = the differential number flux in units of electrons per square centimeter per second per steradian per electronvolt,
- $CNTS$ = the number of pulses from the channeltron counted in the time interval during which the plate voltage was constant,
- ΔT = the accumulation time for the counts during which the plate voltage was constant,
- $G(E_p)$ = the geometric factor at the peak of the response curve in units of square centimeters per steradian, and
- ΔE = the full width at half maximum of the energy-dependent geometric factor.

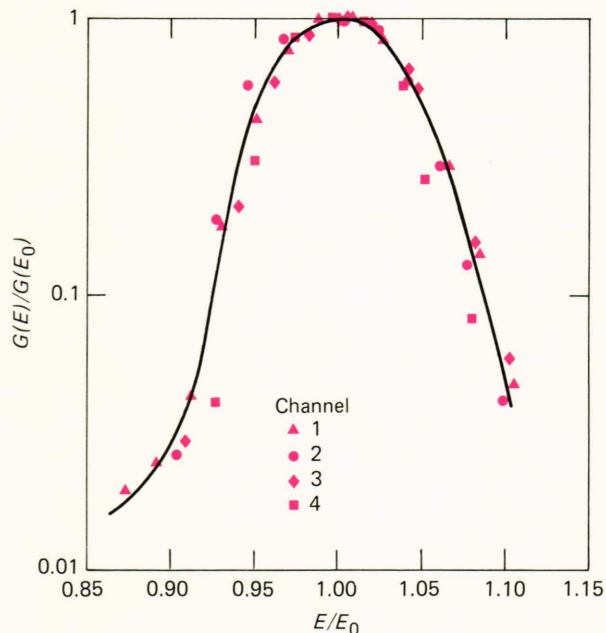


Figure 2—The normalized response curves for the four highest energy channels of the 60° analyzer. The curves have been normalized to the peak response in each channel and to the energy at that peak.

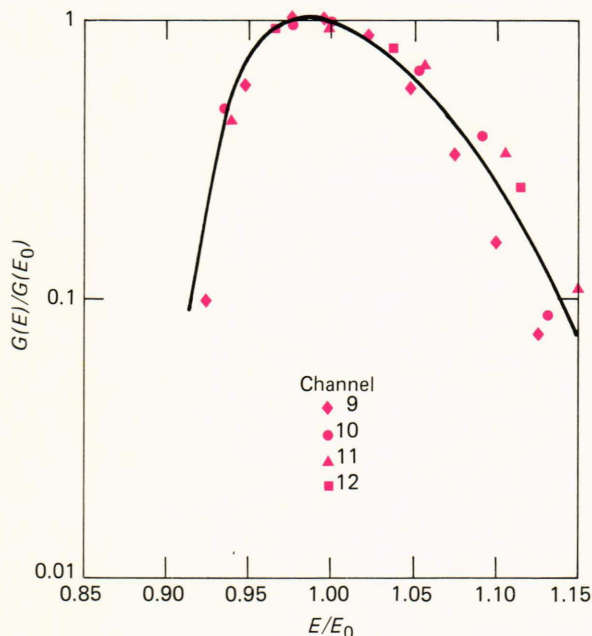


Figure 3—Same as Fig. 2, for the four highest energy channels in the 127° analyzer.

For the 60° assembly, $G(E_p)$ is 10^{-3} cm²/steradian and the $\Delta E/E_p$ is approximately 9%. For the 127° detectors, the two values are 4×10^{-4} square centimeter per steradian and the $\Delta E/E_p$ is approximately 13%.

The complete J sensor with the cover is shown in Fig. 4. The three pairs of analyzers are oriented so that when the experiment is mounted on the satellite, one

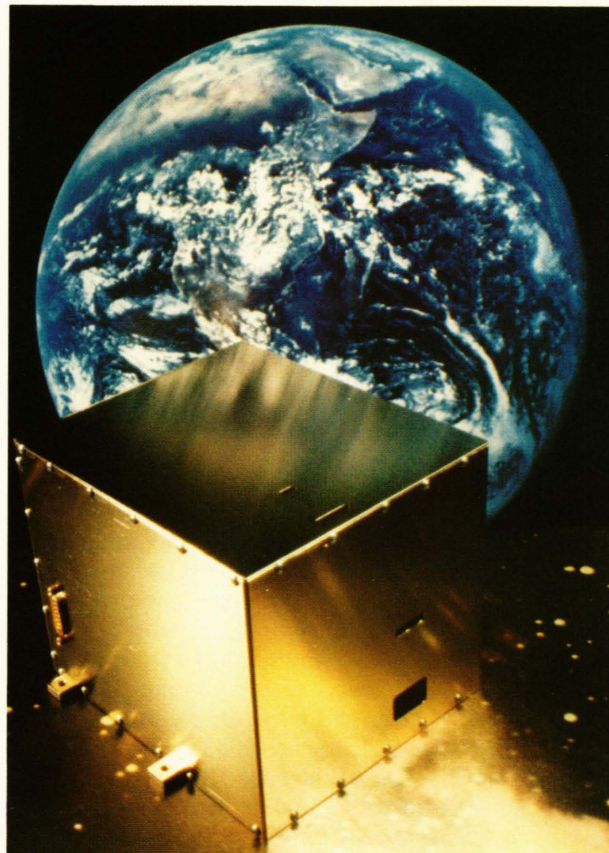


Figure 4—The assembled HILAT J sensor.

pair measures electrons incident from the local zenith, one pair from an angle 40° from the local zenith, and one from the local nadir.

MODES

In order to provide data at a variety of spatial scales, the J sensor was designed with three operating modes:

1. In mode 1, only the channels of the zenith analyzer, measuring between 20 and 632 eV, are sampled. Twenty-four 8-point spectra over this energy range are obtained each second, providing a spatial resolution between consecutive measurements of approximately 300 meters.
2. In mode 2, the channels of both zenith analyzers are sampled. This provides twelve 16-point spectra over the energy range from 20 to 20,000 eV and a spatial resolution of approximately 600 meters.
3. In mode 3, the channels of both analyzers in all three pairs are sampled. This provides four 16-point spectra over the energy range from 20 to 20,000 eV each second in all three directions and a spatial resolution of approximately 1.8 km.

The J sensor is commanded into these modes by a series of consecutive mode commands. A single mode-command sequence delivered to the satellite places the detector in mode 1. Two consecutive sequences of

mode commands sent to the satellite, with the second command arriving within 64 seconds after the first, will switch the J sensor to mode 2. Three mode commands at no greater than 64-second intervals place the sensor in mode 3.

ELECTRONICS

Figure 5 is a simplified functional block diagram of the electronics for the J sensor. The sensor operates as follows: The mode control electronics sets the sensor to one of the three modes described above. The mode electronics are controlled in the manner previously described by the mode command lines and, in turn, control the counter, which divides the frequency of the 4098-hertz spacecraft clock by 2 for mode 1, by 4 for mode 2, or by 12 for mode 3. The resultant frequency clocks the timing and control logic and determines the plate voltage sweep rate to be 24, 12, or 4 sweeps per second. The stepped plate voltage is applied to all six pairs of plates simultaneously. The low-energy plates are driven through a voltage divider at about one-third the level of the high-energy plates. Counts are accumulated in each of the eight levels for 4.026, 9.15, or 29.65 milliseconds in modes 1, 2, and 3, respectively.

The amplified outputs of the channeltron detectors are counted by six 8-bit log counters. Under control of the timing and control logic, these counters accumu-

late counts during the plate voltage dwells. At the end of the accumulation interval, the timing and control logic electronics shift the 8-bit words into one of the two 768-bit shift registers and the log counters are reset to 0. How many of the six log counters are read into the shift register depends on the mode in which the sensor is operating. In mode 1 only the zenith low-energy detector log counter is shifted, in mode 2 the counters for both zenith detectors are shifted, and in mode 3 all six counters are shifted. Which of the two shift registers is to be filled and which is to be read out are controlled by the load and output clocks. The 768-bit shift registers are read out through an 8-bit output shift register. Three analog monitors are sampled sequentially (the temperature, the low voltage powering the electronics, and the high voltage on the plates). The sampling of the high-voltage monitor is synchronized such that sequential voltage steps are sampled. The analog values are fed into an 8-bit analog-to-digital converter whose output is fed in parallel into the output shift register alternately with an 8-bit identification word. The 8-bit identification word tells the operating mode of the J sensor which analog monitor will appear next in the data stream, and, if that analog is a high-voltage measurement, which voltage step is being read out. The 776 bits (768 in the storage register plus 8 in the output register) are finally shifted into the satellite telemetry stream.

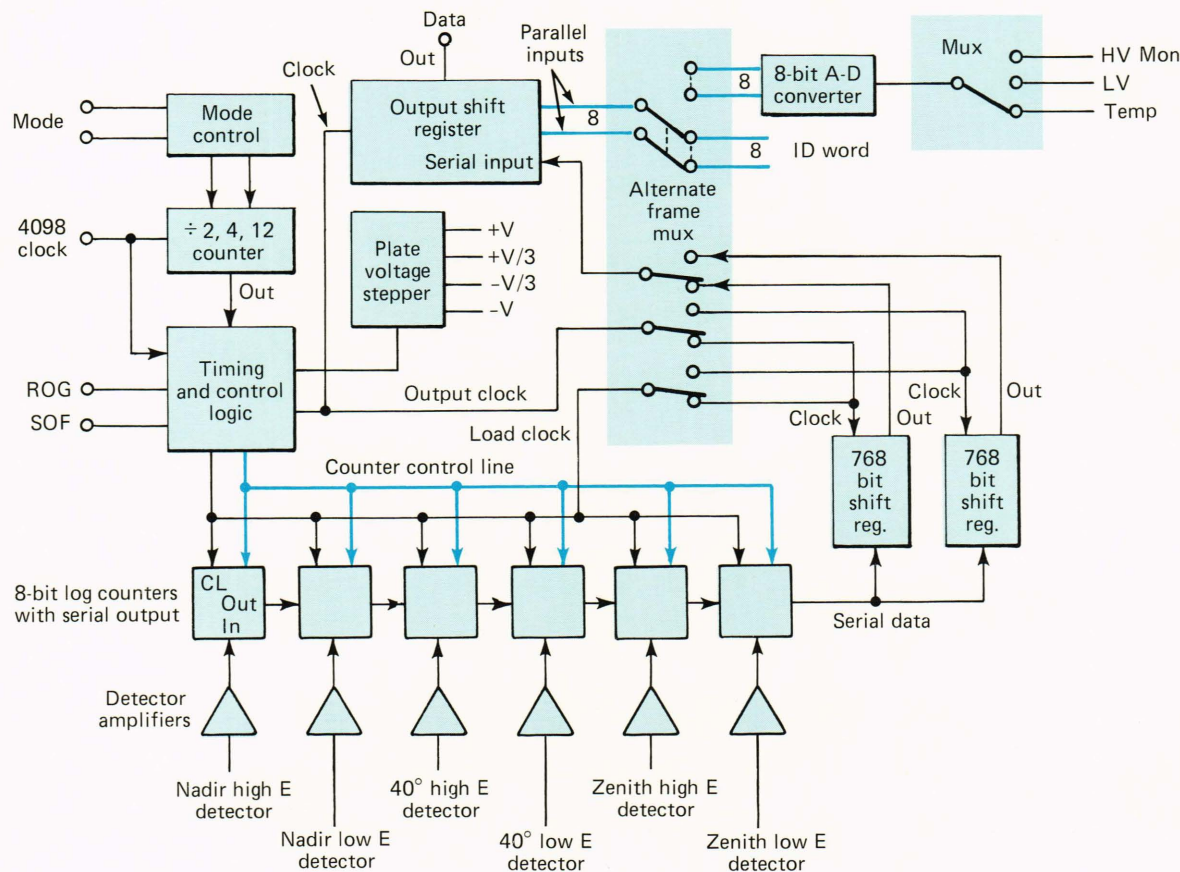


Figure 5—A functional block diagram of the HILAT J sensor electronics.

DATA

The J sensor was operated in orbit for the first time on the evening of July 7, 1983. In the initial check-out, the correct functioning of the detector in all three modes was verified. An example of the early data taken using the receiver at the Applied Physics Laboratory is shown in the color spectrogram format of Fig. 6. These data, from July 17, 1983, are for a period when the J sensor was operating in mode 3. In Fig. 6, the energy of the electrons from 20 to 20,000 eV is plotted along the y axis and time along the x axis. The intensity of the electron precipitation in units of electrons per square centimeter per second per steradian per electronvolt is plotted in a color intensity code, with black as the lowest intensity and white as the highest. Each set of panels gives (from top to bottom) the data from the zenith, 40°, and nadir detectors, respectively. The bottom of Fig. 6 is annotated with the time of the observation (in universal time) and the corrected geomagnetic latitude, longitude, and local time of the satellite.

Data were recorded between 1021:02 and 1031:01 universal time (UT) as the satellite was passing toward the equator along the 0400 magnetic local time meridian. At the beginning of the interval, the sensor is already measuring auroral fluxes. In the zenith and 40° detectors, measurable electron fluxes are observed over the entire energy range up to 20,000 eV for the interval from 1021:02 to 1024:42 UT. In addition, there are two periods in this interval in which peaked spectra are observed (1021:24 to 1021:34 and 1023:12 to 1023:32 UT), as well as numerous increases in the flux of electrons with energies less than approximately 1000 eV. Peaked spectra appear in a color spectrogram as a band of color bounded at both higher and lower energies by colors denoting smaller intensity. The increases in the low-energy electron flux are not seen in the 40° detector because of partial shadowing of the electrons by the satellite, but in the zenith detector they reach values as high as 10^{11} electrons per square centimeter per second per steradian per kiloelectronvolt at 20 eV (at 1022:42, for example). Throughout the

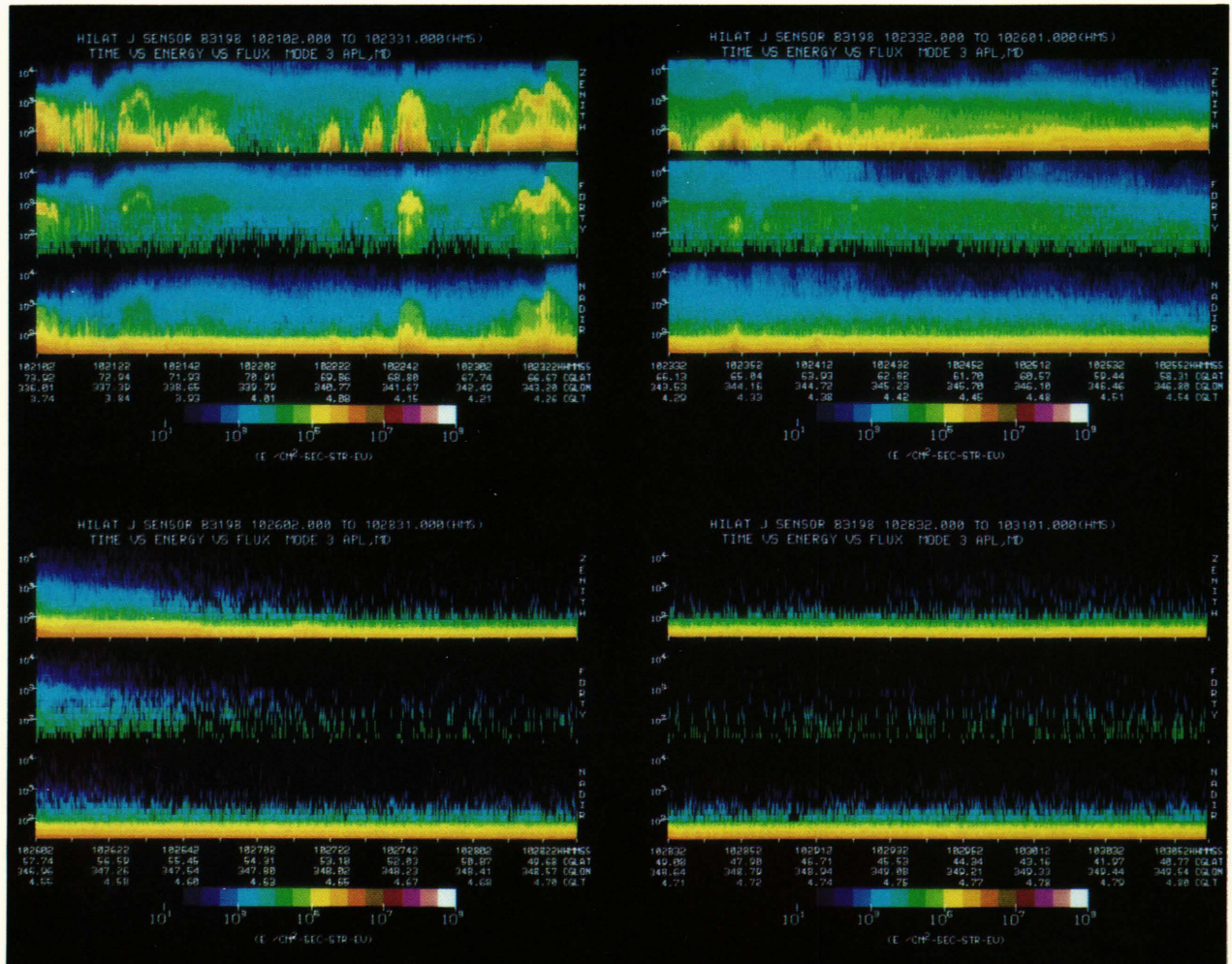


Figure 6—A color intensity spectrogram of the HILAT J sensor data for the time interval between 1021:02 and 1031:01 UT, July 17, 1983. The y axis gives the electron energy, the x axis gives time, and the flux intensity in units of electrons per square centimeter per second per steradian per electronvolt is color coded, with black being the lowest intensity and white the highest.

interval, the nadir detector is measuring a much softer spectrum. This is because the nadir detector is measuring electrons that have interacted with the atmosphere and have been scattered back to the spacecraft. In such a process, the electrons have lost part of their energy.

Between 1024:42 and 1027:22 UT, the electron spectrum decreases in intensity and softens as the satellite passes over the diffuse auroral region and exits the auroral zone. Equatorward of the auroral oval, the majority of the electron flux is produced by photoelectrons with energies below 100 eV. Those seen in the zenith detector were produced in the conjugate hemisphere, then moved along the field line until they reached the satellite position. Those seen in the nadir detector were produced in the ionosphere below the satellite and are moving up the field line. It is interesting to note that the photoelectrons originating below the satellite are more intense than those originating in the conjugate hemisphere.

In Fig. 7, the data for this pass have been plotted in a different format, with each spectrum integrated over energy to give the integral number flux (electrons per square centimeter per second per steradian), the

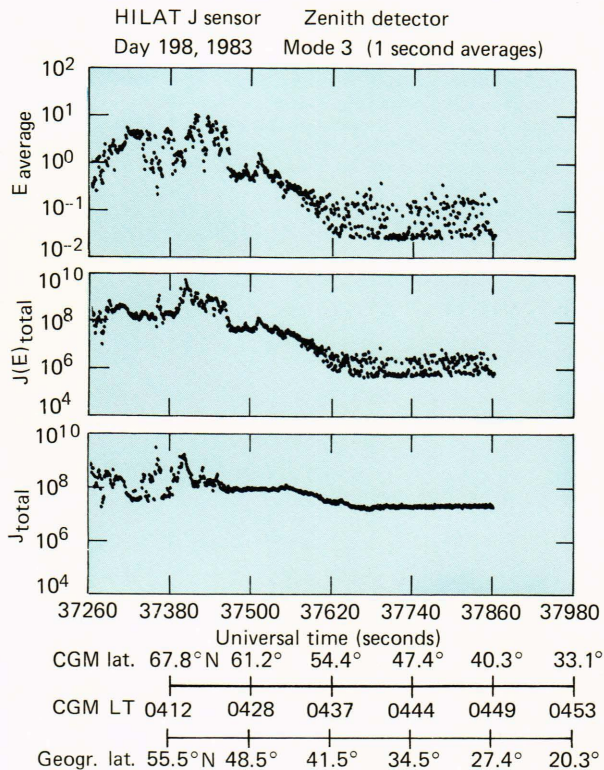


Figure 7—The three panels give, from top to bottom for the zenith measured electron spectra, the average electron energy (in units of kiloelectronvolts), the integrated energy flux (in units of kiloelectronvolts per square centimeter per second per steradian), and the integrated number flux (in units of electrons per square centimeter per second per steradian). The time period covered is the same as in Fig. 6. The bottom of the figure is annotated with the time in universal time (seconds) and the satellite position in corrected geomagnetic and geographic coordinates.

integral energy flux (kiloelectronvolts per square centimeter per second per steradian), and the average energy of the electrons (kiloelectronvolts). These quantities are plotted in three panels from bottom to top, respectively, as a function of time. The bottom of Fig. 7 is annotated with universal time in seconds, the corrected geomagnetic latitude and local time, and the geographic latitude. The figure shows that prior to about 1024:40 UT the electrons are very hot, with average energies near 10 keV. Decreases in the average energy are produced by increases in the flux of low-energy electrons with the largest decrease, to a value less than 100 eV, at about 1022:42, the result of the largest low-energy increase, as was seen in Fig. 6. After 1024:40, the softening and decrease in intensity of the spectrum are seen as a slow falloff in both the average energy and integral number flux.

Figures 8, 9, and 10 show three examples of the differential number flux spectrum for electrons in that pass. Figure 8 is an example of the differential number flux spectrum in the diffuse auroral region. The spectrum smoothly varies with energy, with the flux intensity decreasing slowly with increasing energy. Above 1000 eV, the spectra from the zenith and 40° detectors are approximately the same, while the spectrum from the nadir detector is significantly softer. Figure 9 is an example of an enhancement of the electron flux at low energy. Above about 100 eV, the spectrum has the shape typical of the diffuse aurora. Below 100 eV, the intensity increases sharply, peaking at a value of approximately 3×10^{10} electrons per square centimeter per second per steradian per kiloelectron-

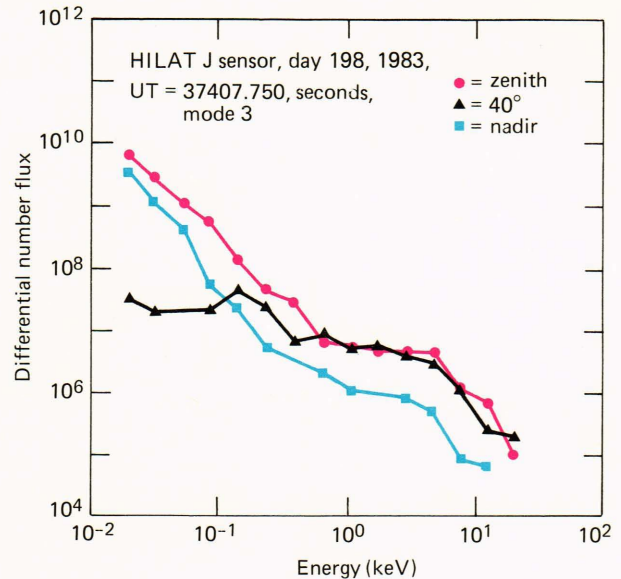


Figure 8—The differential number flux spectra obtained from the HILAT J sensor at 37407.75 seconds UT of July 17, 1983 when the satellite was over the diffuse auroral region. The y axis is in units of electrons per square centimeter per second per steradian per kiloelectronvolt. The x axis is in units of kiloelectronvolts.

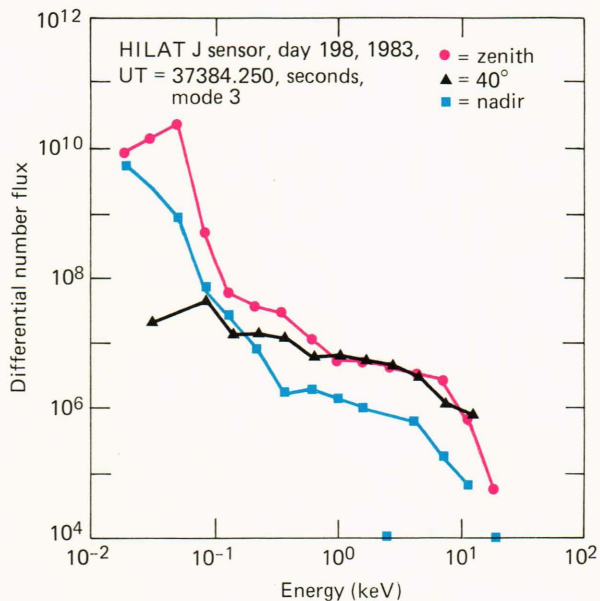


Figure 9—Same as Fig. 8, showing a low energy enhancement.

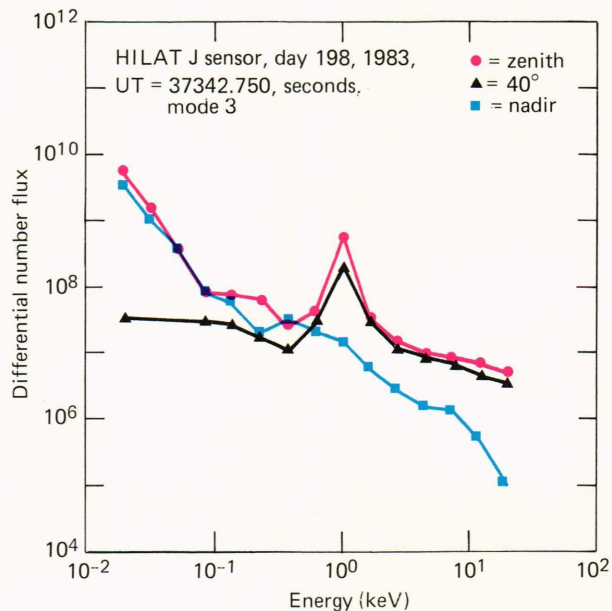


Figure 10—Same as Fig. 8, showing a peaked spectra.

volt at 65 eV. Figure 10 shows a peaked spectrum. In this case the peak is at approximately 1000 eV. Two points are of note: first, the peak appears to be superimposed on a diffuse auroral spectrum, and second, at the peak the flux is somewhat field aligned, with the zenith detector measuring approximately four times the flux of the 40° detector.

NOTE

¹The channeltron is an electron multiplier system consisting of a hollow lead glass tube with a large potential applied between its two ends. Electrons that impact the front end of the channeltron eject secondary electrons. The secondary electrons are accelerated down the tube by the electric field resulting from the applied potential so that, when they collide with the walls of the channeltron, additional secondaries are produced. As the process continues, the resulting electron cascade provides a measurable pulse at the channeltron output that can be counted by the detector electronics.